JOURNAL OF CATALYSIS **177,** 335–342 (1998)
ARTICLE NO. CA982141

Cation/Anion Effects on the Acidic Strengths of the Stoichiometric and Nonstoichiometric Microporous Thallium (I) Salts of 12-Tungstophosphoric, 12-Tungstosilicic, and 12-Molybdophosphoric Acids from the Isomerization of 1-Butene

M. A. Parent and J. B. Moffat[1]

Department of Chemistry and the Guelph-Waterloo, Centre for Graduate Work in Chemistry, University of Waterloo, Waterloo, Ontario, Canada N2L 3G1

Received December 15, 1997; revised April 3, 1998; accepted April 28, 1998

Substitution of protons in 12-tungstophosphoric, 12-tungstosilicic, and 12-molybdophosphoric acids with monovalent thallium cations, representative of group 3B in the periodic table, form high surface area solids which possess a micropore structure. Preparation of the salts with stoichiometric and nonstoichiometric quantities of the cation decreases the concentration of protons remaining in the solid and influences the interactions experienced by these residual protons. Solid state ^{1}H NMR and NH_3 TPD measurements, correlated with catalytic activities observed in the isomerization of 1-butene, have been employed to assess the number of acidic sites, the distribution of acidic strengths, and the effect of changes in the preparative stoichiometry in the three thallium 12-heteropoly oxometalate salts.

INTRODUCTION

The Keggin anion, $(XM_{12}O_{40})^{-n}$, often referred to as a 12-heteropoly oxometalate, is the most frequently studied metal oxygen cluster compound due to its interesting catalytic properties (1). The approximately spherical structure of the Keggin anion can be described as a central atom (X) bonded to four oxygen atoms in a tetrahedral arrangement. This tetrahedron is surrounded by 12 interconnecting octahedra, each consisting of the peripheral metal (M) located at their approximate centres and six oxygen atoms at their vertices. The Keggin anion retains its structure on substitution of different elements for the central and peripheral atoms.

A solid acid is formed when protons balance the charge of the Keggin anion, determined by the oxidation states of the central and peripheral metal atoms, forming a neutral species, $H_nXM_{12}O_{40}$. The acids containing molybdenum are less acidic than those containing tungsten (2) and the latter, for example 12-tungtophosphoric and 12-tungstosilicic acids, have been shown from microcalorimetric measurements with ammonia to have heats of adsorption in the range expected for superacids (3). Experimental work has provided support for these predictions with $H_3PW_{12}O_{40}$ active in the conversion of methanol to hydrocarbons (4) while the partial oxidation of methane to methanol was more effective with the molybdenum analogue (5).

The surface areas of these solid acids are small ($<10\ m^2/g$) (6). Further research in this laboratory has shown, in part from the analysis of nitrogen adsorption–desorption isotherms, that salts of the 12-heteropoly oxometalates prepared with certain of the monovalent cations of group 1A of the periodic table have relatively high surface areas and microporous structures (7). This is a result of the Keggin anions accommodating the larger cations in the lattice by their translation and rotation, thus removing, at least partially, the barriers separating the interstitial voids and creating channels in the solid. Recent work in this laboratory has confirmed that the high surface area, microporous salts are not limited to group 1A elements with similar structures reported for the silver (I) and thallium (I) 12-heteropoly oxometalates (8).

Photoacoustic FTIR studies have shown that protons remain in the precipitated heteropoly oxometalate salts, indicating that the substitution of the protons was incomplete despite the use of a stoichiometric amount of the cation (9) and further work showed that the morphological properties of the salts varied with the relative amounts of the reactants used in their preparation (10). Ammonia TPD and ^{1}H MAS NMR data of the silver (I) and thallium (I) 12-heteropoly oxometalates have provided evidence that the incorporation of nonprotonic cations has an effect on the chemical environment in which the residual protons reside and, thus, on the Brönsted acidity of the salt, which changes with the use of nonstoichiometric quantities of the preparative reagents (8).

[1] To whom correspondence should be addressed. E-mail: jbmoffat@uwaterloo.ca.

0021-9517/98 $25.00

The present work utilizes the temperature-programmed desorption of ammonia, ^{1}H MAS NMR and the isomerization of 1-butene to examine the changes in the number of acid sites and the distribution of acidic strengths in the salts of three 12-heteropoly acids, which differ in acidic properties (12-tungstophosphoric, 12-tungstosilicic, and 12-molybdophosphoric acids), prepared with stoichiometric and nonstoichiometric amounts of thallium (I).

For the last three decades the isomerization of 1-butene has been frequently used as a means of assessing acidic properties of heterogeneous catalysts, to compare the conversion, selectivity and stability of the catalysts (11). Renewed interest in this process has been brought about by the anticipated oversupply of 1-butene, coupled with the demand for *iso*-butylene as an alkene precursor in the synthesis of methyl *tert*-butylether, and a rekindled interest in the mechanism of the isomerization process (12–17).

EXPERIMENTAL

Helium and 1-butene were purchases from Praxair.

The thallium salts of 12-tungstophosphoric, 12-tungstosilicic, and 12-molybdophosphoric acids were prepared as previously described (8). The cation to proton ratios of 0.50, 1.00, and 1.50 were examined for the thallium salt of 12-tungstophosphoric acid (denoted as TlPW, hereafter) while cation to proton ratios of 0.85, 1.00, and 1.15 were prepared for the thallium salts of 12-tungstosilicic and 12-molybdophosphoric acids (denoted as TlSiW and TlPMo, respectively, hereafter). Particle sizes <75 μm were employed. It is important to emphasize that the aforementioned molar ratios refer to the relative amounts of the preparative reagents employed in the synthesis such that, for example, three molar equivalents of the cation were added per mole of HPW for a preparative cation to proton ratio of 1.00.

^{1}H MAS NMR spectra were obtained with a Bruker AMX-500, with an external reference of benzene, at room temperature, and the spinning rate of 7 kHz. Prior to the ^{1}H MAS NMR measurements the salts were heated to 120°C for 1.5 h, allowed to cool to room temperature for 1.5 h, all under a weak vacuum, and stored in a desiccator. The mass of the sample placed in the zirconia holder was recorded prior to each measurement. Infrared spectra were recorded on a Bomen MB-100 FTIR spectrometer. Powder X-ray diffraction patterns were obtained with a Siemens D500 diffractometer using CuKα radiation and a graphite monochromator at 30 mA and 40 kV.

The measurements of nitrogen adsorption–desorption isotherms have been described earlier for these salts (8). The surface areas of the salts were determined by application of the Brunauer–Emmett–Teller (BET) infinite layer equation to the nitrogen adsorption branch of the nitrogen adsorption–desorption isotherms obtained at 77 K. The MP method (18) was employed to generate the distribution of micropore sizes from the adsorption isotherms, while the method of Lecloux and Pirard (19) was used for calibration purposes. The volumes of the micropores (V_{MP}) were estimated from t-plots by extrapolating the linear pressure region of $0.4 < P/P_o < 0.6$ to obtain the *y*-intercept.

For temperature programmed desorption of ammonia the sample was heated to 150°C over a 20-min period with a 20-mL/min flow of helium, after which an aliquot of gaseous ammonia (20 mL) was injected. After one minute, the system was cooled to 30°C over 30 min. The ammonia was desorbed with a temperature ramp of 10°C/min from 30 to 650°C, under a flow of helium (20 mL/min), and monitored by a HP5890 gas chromatograph equipped with a HP5970 mass selective detector.

The catalytic reaction for the isomerization of 1-butene was carried out in a small flow system with a glass tube reactor (6 mm OD, 4 mm ID) of 21 cm in length with a small bubble (15 mm in length, 10 mm OD) placed in its centre, in which the sample of catalyst (150 mg) was supported between two plugs of quartz wool.

The catalyst was pretreated *in situ* in a flow of helium (20 mL/min) at the reaction temperature for 1 h prior to exposure to a mixture of 17% 1-butene: 83% helium, at the same flow rate. The reactant and products were analyzed with a HP 5880A gas chromatograph equipped with a TCD and a Carbopack C column (2 meter $\times$ 1/8″ OD) with the oven temperature set at 50°C. No conversion of 1-butene was observed with an empty reactor in the range of temperatures employed in the present work.

RESULTS

Characterization of Micropore Structure

The characterization of TlPW, TlPMo, and TlSiW salts has been reported previously (8). Infrared spectra show that the structural integrity of the Keggin anion is retained on substitution of the protons by thallium (I) cations. For purposes of illustration the infrared spectrum of TlPW is shown in Fig. 1. The characteristic bands for the Keggin anion between 2000 and 400 cm^{-1} are clearly evident (9a). The triply degenerate asymmetric stretch of the central atom–oxygen bond of the central tetrahedron and the asymmetric stretch of the bond connecting the peripheral metal atom and the terminal oxygen atom are seen at 1078 and 982 cm^{-1}, respectively. Two bands, associated with the peripheral metal–oxygen–peripheral metal bonds, accompanied by some bending character, involve the peripheral atom–oxygen atom bridge between the octahedra in adjacent M_3O_{13} trimetalate units (887 cm^{-1}) and the vibration of the metal–oxygen–metal bridge between octahedra which share edges with one another within the same M_3O_{13} unit (801 cm^{-1}). An additional band results from a combination

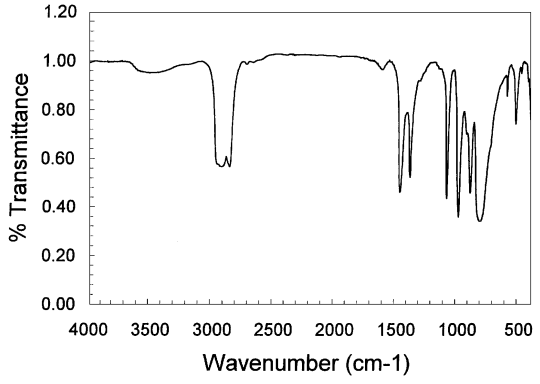

FIG. 1. Infrared spectrum of TlPW with preparative cation/proton ratio of 1.00.

of stretches of the central atom–oxygen bonds, producing deformation in the central tetrahedral unit (596 cm^{-1}). Although shifted slightly, the five characteristic bands for the Keggin anion are present in the infrared spectra for all the thallium salts. Powder X-ray diffraction patterns confirmed that the orientation of the cations and Keggin anions is consistent with the lattice structure present for the acid form of the 12-heteropoly oxometalate.

The microporous structures and surface areas were calculated from the nitrogen adsorption–desorption isotherms, a representative example of which is shown in Fig. 2 (some of the data has been omitted for clarity). The presence of a sharp increase in the quantity adsorbed at small relative pressures is indicative of the presence of micropores and the reversibility of the adsorption branch under desorption conditions demonstrates the absence of mesopores. The surface areas of the salts are summarized in Table 1. For each of the thallium salts examined, at least a 10-fold increase in surface area is apparent when compared to the parent acids, HPW ($S_{BET} = 8\ m^2/g$), HPMo ($S_{BET} = 8\ m^2/g$), and HSiW ($S_{BET} = 4\ m^2/g$) (6). For a given salt, the surface area increases as the relative amount of the cation is increased to a cation : proton ratio of 1.00. The mean micropore radius (r_{MP}) (Table 1) remained virtually unchanged with the amount of cation employed to synthesize the salt, consistent with the hypothesis advanced earlier for the source of the microporous structures in the salts of monovalent cations (7). The micropore volumes are summarized in Table 1 and follow the trend previously discussed with the surface areas, the largest V_{MP} being associated with the stoichiometric salts, again consistent with the earlier hypothesis (7).

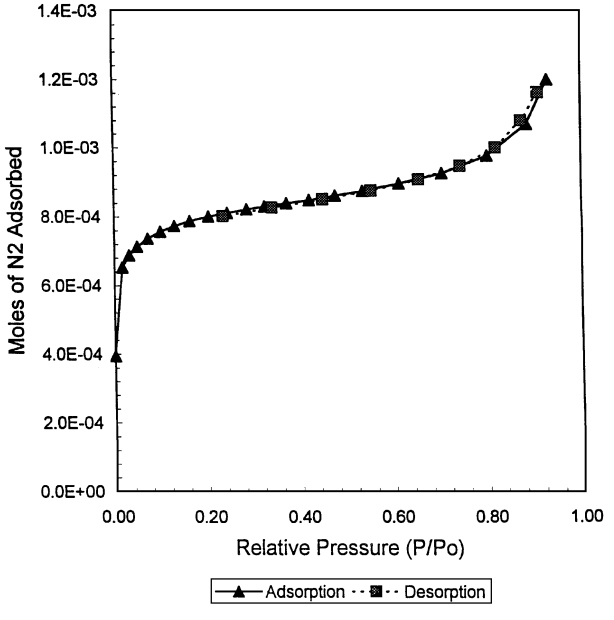

FIG. 2. Nitrogen adsorption–desorption isotherm (77 K) for TlPW with preparative cation/proton ratio of 1.00.

TABLE 1

Surface Areas (S_{BET})[a], Micropore Volumes (V_{MP})[b], and Mean Micropore Radii (r_{MP})[c] of Stoichiometric and Nonstoichiometric Salts

Preparative stoichiometry[d]	TlPW			TlPMo			TlSiW		
	S_{BET}	V_{MP}	r_{MP}	S_{BET}	V_{MP}	r_{MP}	S_{BET}	V_{MP}	r_{MP}
0.50	62.0	0.021	7.6						
0.85	126.9	0.043	8.2	149.7	0.038	8.2	102.5	0.039	7.8
1.00	131.6	0.045	8.2	157.0	0.046	8.4	97.5	0.036	8.0
1.15	128.6	0.043	8.0	147.2	0.041	8.8	92.7	0.035	7.8
1.50	103.6	0.030	7.9						

[a] m^2/g.
[b] mL/g.
[c] Å.
[d] Preparative cation to proton ratio.

Distribution of Acid Sites and Strengths

^{1}H MAS NMR spectra have been obtained for the TlPW, TlPMo, and TlSiW salts. The spectrum for TlPW salts consists of a single resonance, and as the cation to proton ratio increases the relative peak area attributed to the residual protons decreases (Fig. 3). The chemical shifts for protons in HPW has been reported as $\delta = 9.6$ ppm (3). With an increase in the relative amounts of cation used in the synthesis of the salt, the resonance for the residual protons in the TlPW shifts upfield, reflecting a change in the chemical environment of the residual protons (Table 2). In contrast to the TlPW salts, two resonances are present for the residual protons in the TlSiW salts located upfield of the pure acid resonance, noted in the literature as $\delta = 10.9$ ppm (3) (Table 2). The intensities of the two peaks observed exchange as the relative quantities of the cation employed in the salt preparation are increased. The spectra for the three cation to proton ratios of the TlPMo salts mimics the trend observed for the TlPW salts. A single resonance is present in the ^{1}H MAS NMR spectrum, which shifts upfield with the increase in the cation to proton ratio (Table 2). All three

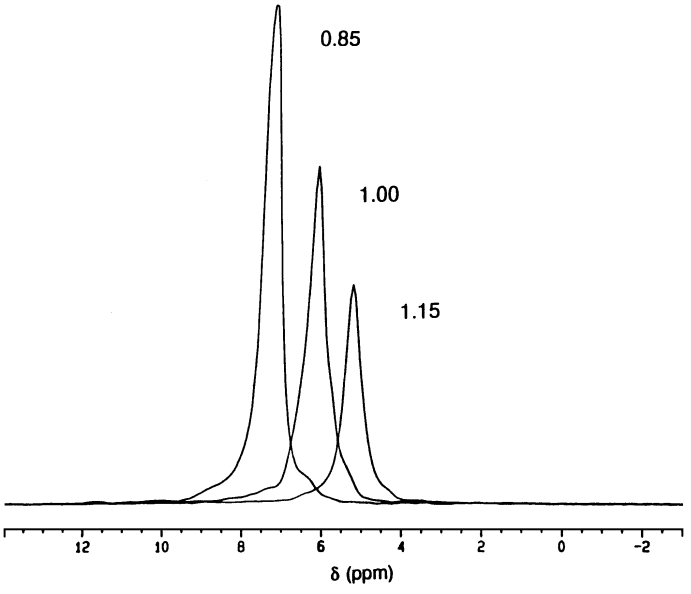

FIG. 3. ^{1}H MAS NMR spectra of TlPW for three preparative cation/proton ratios.

cation to proton ratios depict resonances upfield of those reported for the protons in HPMo, $\delta = 7.4$ ppm (20).

The absolute integrals were measured for each of the ^{1}H MAS NMR spectra. The values obtained for HPW and HPMo, accounting for the amount of the sample measured, were set to be equivalent to three moles of protons per mole of Keggin anion, while the value for HSiW was set to be equivalent to four moles of protons per mole of Keggin anion. The absolute integrals of the salts were then normalized with the value of the parent acid, taking into account the mass of each sample measured. The resulting values confirm that the relative amounts of residual protons decrease with the increase in the relative amounts of cation used in the synthesis with protons present in all samples regardless of the cation to proton ratio (Table 3). As expected, the TlSiW salt has a larger number of protons present as a requirement of the charge balance of the Keggin anion, $SiW_{12}O_{40}^{4-}$, and the solubility limits characteristic of each salt.

TABLE 2

Chemical Shifts (ppm) of Residual Protons for the Stoichiometric and Nonstoichiometric Salts

	Preparative cation to proton ratio		
Salt	0.85	1.00	1.15
TlPW	7.3	6.2	5.2
TlPMo	6.9	6.0	5.3
TlSiW	7.2	6.8[a]	5.6[b]

[a] A shoulder was observed at 6.1 ppm.
[b] A shoulder was observed at 6.2 ppm.

TABLE 3

Composition of Salts Containing Residual Protons

Salt	Cation to proton ratio[a]	H^+/Keggin anion[b]
$H_3PW_{12}O_{40}$		3.0[c]
$H_3PMo_{12}O_{40}$		3.0[c]
$H_4SiW_{12}O_{40}$		4.0[c]
TlPW	0.50	0.46
	0.85	0.41
	1.00	0.26
	1.15	0.15
	1.50	0.16
TlPMo	0.85	0.30
	1.00	0.14
	1.15	0.08
TlSiW	0.85	1.14
	1.00	0.49
	1.15	0.35

[a] Preparative ratio.
[b] Calculated from absolute integrals in ^{1}H MAS NMR data (moles/moles).
[c] Assumed for calibration purposes.

Temperature-programmed desorption (TPD) of ammonia was carried out on the three cation to proton ratios (0.85, 1.00, and 1.15) for each salt examined. Three distinct temperature ranges at which ammonia desorbed were assigned to determine the relative acid strengths: weak (100–300°C), intermediate (300–500°C), and strong (>500°C) acid sites. The total specific acidity for each salt was determined by normalizing the total area recorded for the TPD pattern by the surface area (S_{BET}) and mass of the sample (Table 4). Three peaks are present in the TPD pattern for the 0.85 TlPW salt, with the largest peak appearing at approximately 580°C. The pattern for the stoichiometric TlPW salt shows a very weak peak at approximately the same temperature, but significantly less ammonia is present on this salt than that made with a deficit of the cation. With the TlPW salt having an excess of thallium, a significant difference occurs with the most intense peak at the lowest temperature, as reflected in the distribution in Table 4, and a gradual decline in intensity as the temperature increases. Two shoulders are present on the higher temperature side of the peak, but a peak at greater than 500°C is now absent.

The TlPMo salts made with a deficit and stoichiometric amount of thallium have similar TPD patterns with the major peak at approximately 440°C. This is reflected in the distribution of acid sites (Table 4). With an excess of the cation, a significant shift occurs with the majority of the ammonia desorbed when a temperature of 300°C has been reached, indicating the loss of the strongest acid sites. The TPD spectra of the TlSiW salts contain the most intense peak at approximately 300°C and a shoulder on the higher

TABLE 4

Distribution of Acid Strengths and Total Acidity[a]

Salt	Cation to proton ratio	Acid strength distribution[b] (% of total area)			Total specific acidity[c,d]
		Weak	Intermediate	Strong	
TlPW	0.85	33	29	38	6.0
	1.00	15	43	42	1.2
	1.15	58	31	11	4.7
TlPMo	0.85	36	55	8	5.9
	1.00	31	55	14	3.7
	1.15	68	23	9	2.0
TlSiW	0.85	43	38	18	4.7
	1.00	28	50	22	1.2
	1.15	62	27	11	2.9

[a] Calculated from temperature-programmed desorption of ammonia.
[b] Temperature ranges used for acid strength: weak (100–300°C); intermediate (300–500°C); strong (>500°C).
[c] Total Specific Acidity = Total Area Count/(S_{BET} × mass of sample).
[d] Values multiplied by ($\times 10^8$).

temperature side of this peak declines as the cation to proton ratio is increased. With an excess of thallium, the lowest temperature regions accounts for most of the acid sites (Table 4).

Isomerization of 1-Butene

Isomerization of 1-butene with the thallium salts of 12-tungstophosphoric, 12-molybdophosphoric, and 12-tungstosilicic acids was carried out at 100, 200, and 300°C, with the cation to proton ratios of 0.50, 1.00, and 1.50 for TlPW and ratios of 0.85, 1.00, and 1.15 for the TlPMo and TlSiW salts. The activity of the catalyst was measured at 10 min after exposure to the reagent. The only products formed were the *cis* and *trans* isomers of 2-butene.

As the cation to proton ratio with a given anion increases, the conversions decrease, regardless of the temperature (Table 5). Although the increase of the reaction temperature from 100°C to either 200 or 300°C minimizes the difference in conversions observed for the deficit and stoichiometric salts, the TlPW and TlSiW salts prepared with an excess of the cation display no activity at each of the three reaction temperatures.

For the three series of salts, the ratio of the *cis*/*trans* isomers of 2-butene increases with the increase in the cation to proton ratio, at each temperature. The magnitude of this change is dependent both on the reaction temperature employed and the nature of the Keggin anion.

DISCUSSION

^{1}H MAS NMR has provided evidence that residual protons are still present in the isolated salts. Previous photoacoustic (PAS) FTIR studies have shown that the substitution of protons by larger monovalent cations in precipitated salts, prepared as stoichiometric, was incomplete and protons still remained in the isolated solid (9). For the series of TlPW and TlPMo salts, the protons apparently reside in a single chemical environment with the NMR peak area decreasing as the cation to acid ratio is increased. The chemical shifts of the pure acids, $H_3PW_{12}O_{40}$ and $H_3PMo_{12}O_{40}$ are $\delta = 9.6$ ppm and $\delta = 7.4$ ppm, respectively (3, 20). With the increase of the cation : proton ratio in the TlPW salts, the resonance moves upfield to a smaller chemical shift.

For the TlSiW salts synthesized from 12-tungstosilicic acid, two resonances are present in the ^{1}H MAS NMR spectra, although in most cases, the second peak appears as a shoulder on a more intense peak, disappearing when an excess of the cation is used in the synthesis of the salt. All of the chemical shifts reported for the observed resonances are smaller than that reported for the pure acid, $H_4SiW_{12}O_{40}$, $\delta = 10.9$ ppm (3), and gradually shift further upfield as the cation to acid preparative ratio is increased.

The smaller chemical shift, as compared to the parent acid, and the upfield shift with the increase in the cation to proton ratio indicates that both the nature and quantity of cations, relative to the number of protons, are affecting the chemical environment of the residual protons and, thus, their Brönsted acidity. A number of arguments has been presented in support of the suggestion that the chemical shift can serve as a measure for acid strength (21) and it is generally believed that an increase in the protium chemical shift is an indication of an increase in the Brönsted acid strength (22, 23). The intensity of the resolved line in the ^{1}H MAS NMR spectrum is directly proportional to the concentration of Brönsted acid sites (23). From these results it is apparent that the decrease in chemical shift (Table 2) and peak area (Table 3) as the cation to proton ratio increases is

TABLE 5

Isomerization of 1-Butene at 10 min

Salt	Cation to proton ratio	Conversion (%)			*Cis*/*trans* ratio of 2-butene		
		100[a]	200	300	100[a]	200	300
$H_3PW_{12}O_{40}$		70	86	82	0.361	0.498	0.611
$H_3PMo_{12}O_{40}$		5	9	4	1.231	1.138	0.976
$H_4SiW_{12}O_{40}$		85	85	81	0.372	0.561	0.613
TlPW	0.50	88	87	82	0.366	0.545	0.654
	1.00	25	87	83	1.312	0.575	0.655
	1.50	0	0	0	—	—	—
TlPMo	0.85	28	59	57	0.965	1.067	1.056
	1.00	12	39	53	1.856	1.418	1.209
	1.15	0	23	25	—	1.634	1.528
TlSiW	0.85	34	67	82	1.889	0.810	0.656
	1.00	2	32	71	1.912	1.652	0.891
	1.15	0	0	0	—	—	—

[a] Reaction temperature (°C).

indicative of a decrease in both the number and acid strength of the residual protons as compared to 12-heteropoly acids. This is in agreement with previous work with zeolites (24). The acid strength of the zeolites decreased on exchange of the protons with metallic cations with the stronger acid sites exchanging first.

All three thallium salts have a 1.6 ppm, or greater, difference in chemical shift between the salts with a deficit and an excess of the cation. This change in the protium environment is reflected in the temperature programmed desorption spectra of ammonia with a decrease in the proportion of strong acid sites as the cation to proton ratio for the salts is increased (Table 4). Evidently the distribution of acid strength is shifting with the numbers of sites of higher acidity decreasing as the relative quantities of the cations are increased. Although temperature-programmed desorption experiments with ammonia cannot differentiate between Lewis and Brönsted acid sites, previous photoacoustic FTIR studies have shown that the acidity of 12-tungstophosphoric acid can be attributed to Brönsted acid sites with little or no evidence of Lewis acid sites (9a). It is expected that the derivatives prepared in the present work are similar in this respect.

Isomerization of 1-butene by the salts was carried out to gain an understanding of the number and nature of acid sites available in the catalyst by analysis of the conversion levels and product distribution, in comparison to that of the parent acid. The monomolecular mechanism appears to be followed with the formation of the secondary butyl carbenium ion as the initial step. From this carbenium ion double bond isomerization will form the *cis* and *trans* isomers of 2-butene while skeletal isomerization will form *iso*-butene provided that sites of sufficient acidic strength are present and other conditions are suitable. Recent experiments in this laboratory (11) have indicated that an equilibrium is established between the secondary carbenium ion, 1-butene, *cis*- and *trans*-2-butenes and suggests that the 2-butenes are precursors to *iso*-butene, with the former species as the primary products and *iso*-butene as a secondary product. Stronger Brönsted acid sites and an increase in temperature are required to facilitate the skeletal rearrangement of the secondary butyl carbenium ion to a *tert*-butyl carbenium ion required for this product. This is in agreement with other work which showed that skeletal isomerization could be suppressed while maintaining activity for the linear isomers, indicating that skeletal isomerization requires a different active site than that involved in linear isomerization (25). A decrease in *iso*-butene also correlated with a decrease in the byproduct formation, indicating the latter is formed by a consecutive reaction (25).

Semiempirical quantum mechanical (extended Hückel) calculations have predicted that solid heteropoly acids with anions containing tungsten should have higher acid strengths than those with molybdenum (2). Isomerization of 1-butene with various 12-heteropoly acids revealed that the level of activity for the acid was not affected by changing the central atom in the Keggin anion, in contrast with the observations where the peripheral metal element was changed (27). This is consistent with the results observed for the three 12-heteropoly acids investigated in this work. HPW and HSiW had similar conversions at each of the three reaction temperatures studied, although HPW deactivated more rapidly than HSiW at 100°C. In contrast, little or no activity was observed for HPMo, even at temperatures as high as 300°C. This pattern was not maintained after the partial substitution of protons by the monovalent cations of thallium.

The decrease in activity for the salts at 100°C as the cation to proton ratio increases indicates the number of acid sites of sufficient strength to facilitate the reaction is decreasing. With the increase of the reaction temperature to 200 or 300°C, the TlPW salts maintain similar conversion levels to that observed with HPW. In comparison, the thallium salts of HSiW were not able to achieve a similar degree of conversion for the isomerization of 1-butene as that observed with the parent acid, even at reaction temperatures as high as 300°C. Unlike the analogous TlSiW and TlPW salts, reaction temperatures of 200 and 300°C are sufficiently high to generate nonzero conversions with 1.15 TlPMo. In all cases, the thallium salts have a higher activity than observed for the parent acid, HPMo.

In all of the reactions carried out with the thallium salts of HPW, HSiW, and HPMo, only the *cis* and *trans* isomers of 2-butene were formed. No evidence of C_3, C_4, C_5, . . . , C_8 species was present to give an indication of a bimolecular process. None of the catalysts investigated possessed sites of sufficient strength to facilitate the skeletal isomerization required to form *iso*-butene during the isomerization of 1-butene at the reaction temperatures investigated. This is not surprising since both the ^{1}H MAS NMR and TPD experiments with ammonia revealed that there is a decrease in the Brönsted acidity with the increased substitution of cations in comparison to the pure acid. Although isomerization of 1-butene at 300°C by 12-tungstophosphoric acid did not produce *iso*-butene, supported HPW was capable of forming *iso*-butene during the isomerization of 1-butene at these temperatures (11). ^{1}H MAS NMR studies of the supported acid revealed a downfield movement of the protium resonance, to a larger chemical shift from that reported for the unsupported HPW, indicating an increase in acid strength when the acid is supported (11). With the supported HPW, there was also evidence of a bimolecular process under the reaction conditions employed, but this may be restricted to the formation of the byproducts (25).

Formation of the *cis* and *trans* isomers of 2-butene occurs through the secondary butyl carbenium ion, which is considered to be a metastable species, not equivalent to a transition state (28). A ratio of 1 is expected for the *cis*/*trans*

isomers from this carbenium ion since the activation energy to form either is identical, although the *trans* isomer is slightly more thermodynamically stable. For 1-butene isomerization, this ratio is expected when the reaction is limited kinetically and the intermediate secondary butyl carbenium ion is considered to be "free" (29). However, the equilibrium distribution of 1-butene : *cis*-2-butene : *trans*-2-butene is 9.3 : 29.8 : 60.9 at 150°C (30), giving a *cis*/*trans* ratio of 0.49, and 18.0 : 32.5 : 49.5 with a *cis*/*trans* ratio of 0.656 at 300°C (31). Isomerization of 1-butene with HPW and HSiW acids results in *cis*/*trans* ratios similar to the equilibrium distribution values (Table 5) for reaction at 100°C slightly lower than the distribution reported for 150°C. The *cis*/*trans* ratio obtained with HPMo were close to values of 1.0 at 300°C, but increased as the reaction temperature decreased (Table 5).

The TlPW salt prepared with a deficit of the cation produced the two isomers of 2-butene in ratios similar to the equilibrium values. However, with the stoichiometric salt a *cis*/*trans* ratio significantly higher than the equilibrium value was observed. Increasing the reaction temperature decreased the selectivity for the *cis* isomer with equilibrium values being found for reactions performed at 300°C. For the TlSiW salts, reactions at 100°C produced *cis*/*trans* ratios of approximately 2, but these decreased and approached the values expected at equilibrium as the reaction temperature increased. The TlPMo salts mimic the pattern observed with the other thallium salts, with the fraction of *cis*-2-butene produced increasing as the thallium content of the salt is increased. Reactions at 100°C show the greatest range in the *cis*/*trans* ratio, although all ratios are greater than 1, higher than observed for the pure acid.

With the isomerization reactions carried out with the pure 12-heteropoly acids the formation of the *cis* isomer has been suggested as favourable for catalysts which are weakly acidic (27). This had previously been noted with other catalysts (13, 26) although numerical values reported for the *cis*/*trans* ratio are largely dependent upon the nature of the acid sites (Lewis or Brönsted) and the resulting mechanism for isomerization. This is consistent with the observations for the ammonia TPD, in which a greater portion of acid sites are classified as weak with the increase in the cation to proton ratio for the three series of thallium salts examined.

As evident from the nitrogen adsorption–desorption isotherms, ^{1}H MAS NMR and ammonia TPD, partial substitution of the protons by thallium cations affects three characteristics of the salts: a microporous structure is created, the number of Brönsted acid sites is decreased, and the distribution of acid sites is shifted. As noted earlier, variations in the cation to proton ratios have significant effects on the pore volumes but little or no influence on the mean micropore radius, as would be expected from the hypothesis of the source of the pore structure advanced earlier (6). Not surprisingly, however, the number of residual protons and the chemical environment in which they reside are altered by changes in this ratio. With respect to the isomerization of 1-butene, the change in the distribution of acid sites for the thallium salts is reflected in both the conversion and the product distribution of the two isomers of 2-butene formed.

It is evident that four factors play significant roles in influencing the isomerization of 1-butene: (1) the nature of the anion, (2) the morphological properties of the catalyst, (3) the number of protons, and (4) the distribution of acid strengths. For a given cation and anion, the latter three factors are determined by the preparative stoichiometry of the catalyst. To elucidate the effect of the cations on the protons and the distribution of acid strengths, the conversions were divided by the appropriate surface areas and numbers of protons (Table 6). The resulting quantities should substantially reduce or eliminate the effect of the numbers of protons and morphological differences among the catalysts on the observed conversions.

Two general trends are evident in Table 6. With TlPW and TlSiW the specific conversion at a given temperature decreases to insignificant values as the cation to proton ratio is increased. In contrast, with TlPMo the specific conversion at each of the two higher temperatures increases with the cation : proton ratio. Evidently the salt containing molybdenum is influenced in a diametrically opposed manner on the introduction of thallium rather than those containing tungsten.

The semiempirical quantum mechanical calculations which determined the sequence of acidic strengths for the heteropoly acids indicated that the negative charge on the terminal oxygen atoms in the Keggin anions has an effect on the mobility of the protons, and thus the acidity of the heteropoly acid (2). Changing the peripheral metal atoms from tungsten to molybdenum would increase the coulombic

TABLE 6

Conversion of 1-Butene at 10 min with Thallium Salts

Salt	Cation to proton ratio	Conversion[a,b,c]/[(m^2)(H^+)]		
		100[d]	200	300
TlPW	0.50	8.9	7.4	5.9
	1.00	9.0	3.6	1.4
	1.50	0.0	0.0	0.0
TlPMo	0.85	0.8	1.3	1.4
	1.00	0.6	2.3	2.9
	1.15	0.0	3.0	3.6
TlSiW	0.85	0.5	1.9	0.8
	1.00	0.1	1.8	1.9
	1.15	0.0	0.0	0.0

[a] For measurements taken at 10 min.
[b] Moles of products multiplied by (1×10^{26}).
[c] Relative number of protons from ^{1}H MAS NMR data.
[d] Reaction temperature (°C).

binding of the proton as the charge on the terminal oxygen atoms is increased, while protonic mobility and acidity will decrease. It appears that the introduction of larger cations into the lattice structure with the Keggin anions also alters the mobility of the protons. The larger size and repulsive interactions of the cations could restrict the physical movement of the protons. In addition, the nonprotonic cations may perturb the electron densities of the anions, altering the magnitude of the charge on the terminal oxygen atoms.

The introduction of a larger cation, thallium in the present context, apparently has a qualitatively dissimilar effect with the tungsten- and molybdenum-containing salts. With the former the distribution of acidic strengths is shifted to lower values, while with the latter higher values are attained. The influence of the larger cation thus appears to be dependent on the magnitude of the charge on the terminal oxygen atoms, producing a beneficial effect where the magnitude is high and a disadvantageous effect with low magnitudes. Where the acidic strength of the parent acid is relatively low the introduction of larger cations enhances the acidity, whereas with the stronger parent acids the acidity is apparently depressed.

It should be noted that while these interpretations are speculative, the influence of the larger nonprotonic cations on the acidic properties of the heteropoly acids as a result of direct and/or indirect interactions of the protons and the cations is evident.

ACKNOWLEDGMENTS

The financial support of the National Sciences and Engineering Research Council of Canada through Operating, Equipment and Industrially Oriented Research Grants, the Province of Ontario through its University Research Incentive fund and Imperial Oil through the Environmental Science and Technology Alliance Canada is gratefully acknowledged.

REFERENCES

1a. Pope, M. T., "Heteropoly and Isopoly Oxometalates," Springer-Verlag, Berlin, 1983.
1b. Pope, M. T., and Müller, A., *Angew. Chem. Int. Ed. Engl.* **30**, 34 (1991).
2. Moffat, J. B., *J. Mol. Catal.* **26**, 385 (1985).
3. Jozefowicz, L. C., Karge, H. G., Vasilyeva, E., and Moffat, J. B., *Microporous Mater.* **1**, 313 (1993).
4. Hayashi, H., and Moffat, J. B., *J. Catal.* **77**, 473 (1982).
5a. Kasztelan, S., and Moffat, J. B., *J. Catal.* **106**, 512 (1987).
5b. Moffat, J. B., and Kasztelan, S., *J. Catal.* **109**, 206 (1988).
5c. Kasztelan, S., Payen, E., and Moffat, J. B., *J. Catal.* **125**, 45 (1990).
6. Moffat, J. B., *J. Mol. Catal.* **52**, 169 (1989).
7a. McMonagle, J. B., and Moffat, J. B., *J. Colloid Interface Sci.* **101**, 479 (1984).
7b. Taylor, D. B., McMonagle, J. B., and Moffat, J. B., *J. Colloid Interface Sci.* **108**, 278 (1985).
7c. McGarvey, G. B., and Moffat, J. B., *J. Colloid Interface Sci.* **125**, 15 (1988).
7d. McGarvey, G. B., and Moffat, J. B., *J. Catal.* **130**, 483 (1991).
7e. Bonardet, J. L., McGarvey, G. B., Moffat, J. B., and Fraissard, *J. Colloid Surf. A* **72**, 191 (1993).
7f. Bonardet, J. L., Fraissard, J., McGarvey, G. B., and Moffat, J. B., *J. Catal.* **151**, 147 (1995).
7g. Bonardet, J. L., Carr, K., Fraissard, J., McGarvey, G. B., McMonagle, J. B., Seay, M., and Moffat, J. B., *in* "Advanced Catalysis and Nanostructured Materials" (W. R. Moser, Ed.), p. 395. Academic Press, San Diego, 1996.
8. Parent, M. A., and Moffat, J. B., *Langmuir* **12**, 3733 (1996).
9a. Highfield, J. G., and Moffat, J. B., *J. Catal.* **88**, 177 (1984).
9b. Highfield, J. G., and Moffat, J. B., *J. Catal.* **89**, 185 (1984).
9c. Highfield, J. G., and Moffat, J. B., *J. Catal.* **95**, 108 (1985).
9d. McGarvey, G. B., and Moffat, J. B., *J. Catal.* **128**, 69 (1991).
10. Lapham, D., and Moffat, J. B., *Langmuir* **7**, 2273 (1992).
11. Gao, S., and Moffat, J. B., *Catal. Lett.* **42**, 105 (1996) (and references therein).
12. Houzvicka, J. H., Klik, R., Kubelkova, L., and Ponec, V., *Appl. Catal. A* **150**, 101 (1997).
13. Béres, A., Pálinkó, I., and Kiricsi, I., *React. Kinet. Catal. Lett.* **59**, 47 (1996).
14. Xu, W.-Q., Yin, Y.-G., Suib, S. L., Edwards, J. C., and O'Young, C.-L., *J. Catal.* **163**, 232 (1996).
15. Meriaudeau, P., Bacaud, R., Ngoc Hung, L., and Vu, A. T., *J. Mol. Catal. A* **110**, L177 (1996).
16. Houzvicka, J., and Ponec, V., *Appl. Catal. A* **145**, 95 (1996).
17. Aseni, M. A., Corma, A., and Martinez, A., *J. Catal.* **158**, 561 (1996).
18. Mikhail, R. Sh., Brunauer, S., and Bodor, E. E., *J. Colloid Interface Sci.* **26**, 45 (1968).
19. Lecloux, A., and Pirard, J. P., *J. Colloid Interface Sci.* **70**, 265 (1979).
20. Matikhin, V. M., Kulikov, S. M., Nosov, A. V., Kozhevnikov, I. V., Mudrakovsky, I. L., and Timofeeva, M. N., *J. Mol. Catal.* **60**, 65 (1990).
21. Pfeifer, H., Freude, D., and Karger, J., *Stud. Surf. Sci. Catal.* **65**, 89 (1991).
22. Pfeifer, H., *in* "Acidity and Basicity of Solids: Theory, Assessment and Utility" (J. Fraissard and L. Petrakis, Eds.), p. 255. Kluwer, Dordrecht, 1994.
23. Freude, D., Ernst, H., Mildner, T., Pfiefer, H., and Wolf, I., *Stud. Surf. Sci. Catal.* **90**, 105 (1993).
24. Barthomeuf, H., *Stud. Surf. Sci. Catal.* **65**, 157 (1991).
25. Gielgens, L. H., van Kampen, M. G. H., Broek, M. M., van Hardeveld, R., and Ponec, V., *J. Catal.* **154**, 201 (1995).
26. Vaughan, J. S., Conner, C. T. O., and Fletcher, J. C. Q., *J. Catal.* **147**, 441 (1994).
27. Matsuda, T., Sato, M., Kanno, T., Miura, H., and Sugiyama, K., *J. Chem. Soc. Faraday Trans I* **77**, 3107 (1981).
28a. Hightower, J. W., and Hall, W. K., *J. Phys. Chem.* **71**, 1014 (1967).
28b. Hightower, J. W., and Hall, W. K., *Chem. Eng. Prog. Symp. Ser.* **63**, 122 (1967).
28c. Hightower, J. W., and Hall, W. K., *J. Amer. Chem. Soc.* **89**, 778 (1967).
29. Patrono, P., La Ginestra, A., Ramis, G., and Busca, G., *Appl. Catal. A* **107**, 249 (1994).
30a. Makarova, M. A., Paukshtis, E. A., Thomas, J. M., Williams, C., and Zamaraev, K. I., *J. Catal.* **149**, 36 (1994).
30b. Zamaraev, K. I., and Thomas, J. M., *in* "Advances in Catalysis," (D. D. Eley, W. O., Haag, and B. Gates, Eds.), Vol. 41, p. 335. Academic Press, San Diego, 1996.
31. Voge, H. H., and May, N. C., *J. Amer. Chem. Soc.* **68**, 550 (1946).